International Symposium
On Turbulence and Shear Flow
Phenomena (TSFP-9)
June 30 - July 3, 2015 *Melbourne, Australia*

APPLICATION OF SCALE SIMILARITY BASED MODELS TO SUBGRID SCALE SCALAR FLUX MODELLING IN THE CONTEXT OF TURBULENT PREMIXED FLAMES

Markus Klein
Department of Aerospace Engineering, Universität der Bundeswehr München,
Werner-Heisenberg-Weg 39, 85577 Neubiberg, Germany
markus.klein@unibw.de
Nilanjan Chakraborty, Yuan Gao
School of Mechanical and Systems Engineering, Newcastle University,
Newcastle-Upon-Tyne, NE1 7RU, UK
nilanjan.chakraborty@newcastle.ac.uk, yuan.gao2@ncl.ac.uk

ABSTRACT

A variety of closures for sub-grid (SGS) scalar flux in the context of Large Eddy Simulations (LES) of premixed turbulent combustion has been assessed in this work. Besides well-known scale similarity (SS) type models a new development of Anderson and Domaradzki (2012) is included in the analysis together with two conventional models of reactive scalar flux closure. The work is based on a priori analysis of two Direct Numerical Simulation (DNS) databases of freely propagating turbulent premixed flames with a range of Lewis numbers and turbulent Reynolds numbers. The sub-grid scalar flux exhibits both local gradient and counter-gradient transport (CGT). The direction of the flux depends on the balance between the effects of flame normal acceleration due to heat release and the effects of turbulent velocity fluctuations (Veynante et al., (1997)), as well as the filter size. The models will first be compared component-wise with the flux evaluated from DNS (denoted vector level analysis). In addition the term $\bar{\rho}(\widetilde{u_i c} - \tilde{u}_i\tilde{c})\partial\tilde{c}/\partial x_i$ will be analyzed because it is responsible for production / destruction of progress variable variance and for the energy transfer between scales by the combined effect of mean gradients and scalar flux (scalar level analysis). Most models analyzed in this work have been developed for momentum transport in non-reactive flows. Nevertheless they show equal or better performance compared to models developed for reactive scalar closure.

PLANAR FLAME DNS DATABASE

Two simple chemistry DNS databases of freely propagating statistically planar turbulent premixed flames have been considered for the current analysis. The first database consists of five flames with global Lewis number Le = 0.34, 0.6, 0.8, 1.0 and 1.2 (denoted cases A1-E1). The initial velocity fluctuation is in all cases $u'/S_L = 7.5$ and the initial turbulent Reynolds number is $Re_t = 49$. The second database consists of five unity Lewis number flames with increasing velocity fluctuation and a range of different initial $Re_t = 22, 23.5, 49, 100, 110$ (denoted cases A2-E2). The initial values of normalized root mean square turbulent velocity fluctuation u'/S_L, the ratio of turbulent integral length scale to flame thickness l/δ_{th}, Damköhler number $Da = lS_L/\delta_{th}u'$, Karlovitz number $Ka = (u'/S_L)^{3/2}(l/\delta_{th})^{-1/2}$ and turbulent Reynolds number $Re_t = \rho_0\, u' l/\mu_0$ are provided in Table 1 where ρ_0 and μ_0 are the unburned gas density and viscosity respectively, $\delta_{th} = (T_{ad} - T_0)/Max\,|\nabla\hat{T}|_L$ is the thermal flame thickness with $\hat{T}$ being the dimensional temperature and the subscript 'L' refers to the unstrained laminar planar flame quantities. It is worth noting that flame-turbulence interaction takes place under decaying turbulence. In all the following figures the u'/S_L values refer to the initial turbulence intensity. For the Lewis (Reynolds) number database the simulation domain is taken to be a cube of $24.1\,\delta_{th} \times 24.1\,\delta_{th} \times 24.1\,\delta_{th}$ ($36.1\,\delta_{th} \times 24.1\,\delta_{th} \times 24.1\,\delta_{th}$) which is discretised using a uniform Cartesian grid of 230×230×230 (345×230×230) points ensuring 10 grid points are kept within the thermal flame thickness δ_{th}. An explicit 10th order accurate finite difference formulation together with a 3rd order Runge-Kutta scheme are used for integrating the conservation equations. Further details are omitted for the sake of brevity and the reader is referred to Chakraborty et al. (2011a,b) for additional information on these databases.

Table 1. Lists of initial simulation parameters and non-dimensional numbers.

Case	A1	B1	C1	D1	E1
Le	0,34	0,6	0,8	1	1,2
u'/S_L	7,5	7,5	7,5	7,5	7,5
l/δ_{th}	2,45	2,45	2,45	2,45	2,45
Da	4,5	4,5	4,5	4,5	4,5
Ka	0,33	0,33	0,33	0,33	0,33

Case	A2	B2	C2	D2	E2
u'/S_L	5.0	6.25	7.5	9.0	11.25
l/δ_{th}	1.67	1.44	2.5	4.31	3.75
Re_t	22.0	23.5	49.0	100	110
Da	0.33	0.23	0.33	0.48	0.33
Ka	8.65	13.0	13.0	13.0	19.5

Instantaneous views of isosurfaces for cases A2 and E2 when the statistics were extracted (i.e. $t = \delta_{th}/S_L$) are shown in Fig. 1.

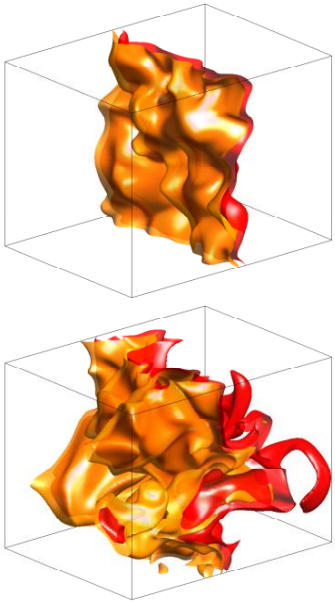

Figure 1. Instantaneous view of c isosurfaces for cases A2 and E2 at $t = \delta_{th}/S_L$. The value of c increases from 0.1 to 0.9 from yellow to red.

MODEL FORMULATIONS

The most conventional model for the SGS scalar flux $h_i = \overline{\rho u_i c} - \bar{\rho}\widetilde{u_i}\tilde{c}$ ($\tilde{}$ denotes Favre filtering) of a reaction progress variable c is the gradient hypothesis model (GHM), which takes the following form for $C_s = 0.18, Sc_t = 1.0$:

$$h_i^{\mathrm{GHM}} = -\frac{\mu_t}{Sc_t}\frac{\partial \tilde{c}}{\partial x_i}, \quad \mu_t = (C_s\Delta)^2\sqrt{2\,\widetilde{S_{ij}}\widetilde{S_{ij}}} \qquad (1)$$

The standard SS model (denoted VSS) is given by

$$h_i^{\mathrm{VSS}} = \bar{\rho}(\widetilde{u_i c} - \widetilde{u_i}\tilde{c}) = \bar{\rho}\left(\widetilde{\widetilde{u_i}\tilde{c}} - \widetilde{\widetilde{u_i}}\tilde{c}\right) \qquad (2)$$

Writing the filter operation as a Taylor series (see Sagaut,1998) the model can be also written as (denoted CGM, Clarks gradient model):

$$h_i^{CGM} = \bar{\rho}(\widetilde{u_i c} - \widetilde{u_i}\tilde{c}) = \bar{\rho}\frac{\Delta^2}{12}\frac{\partial \widetilde{u_i}}{\partial x_k}\frac{\partial \tilde{c}}{\partial x_k} \qquad (3)$$

Another SS model is the one involving not only filtered velocities as the VSS model but also filtered density (therefore named DSS model) and is according to Vreman (1995) given by the expression:

$$h_i^{\mathrm{DSS}} = \overline{\bar{\rho}\widetilde{u_i}\tilde{c}} - \overline{\bar{\rho}\widetilde{u_i}}\;\overline{\bar{\rho}\tilde{c}}\;/\;\bar{\bar{\rho}} \qquad (4)$$

Anderson and Domaradzki's (2012) modification of the VSS model takes in this context the following form

$$h_i^{\mathrm{ASS}} = -\bar{\rho}\left(\widehat{\bar{\tilde{c}}}\;\widehat{\bar{u}_j} - \widehat{\bar{\tilde{c}}}\;\widehat{\bar{u}_j}\right) - \bar{\rho}\left(\widehat{\tilde{c}}\;\overline{u_j'} - \widehat{\bar{\tilde{c}}}\;\overline{u_j'}\right) \qquad (5)$$

where $\overline{u_j}' \coloneqq \bar{u}_j - \widehat{\bar{u}_j}$. It is noted that 2 test filter levels are required and that in contrast to momentum transport this model is Galilei invariant even for compressible flow. On an empirical basis the following extension (EGM) of the CGM model has been formulated and assessed in this work:

$$h_i^{\mathrm{EGM}} = \bar{\rho}(\widetilde{u_i c} - \widetilde{u_i}\tilde{c}) = \bar{\rho}\frac{\Delta^2}{12}\frac{\partial \widetilde{u_i}}{\partial x_k}\frac{\partial \tilde{c}}{\partial x_k} + 2\frac{\Delta^4}{12^2}\frac{\partial \widetilde{u_i}}{\partial x_k}\frac{\partial \bar{\rho}}{\partial x_k}\cdot\frac{\partial^2 \tilde{c}}{\partial x_k^2} + 2\frac{1}{\bar{\rho}}\frac{\Delta^4}{12^2}\frac{\partial \widetilde{u_i}}{\partial x_k}\frac{\partial \bar{\rho}}{\partial x_k}\cdot\frac{\partial \tilde{c}}{\partial x_k}\frac{\partial \bar{\rho}}{\partial x_k} \qquad (6)$$

Finally a model typically used in the context of premixed turbulent combustion is due to Richard et al. (2007):

$$h_i^{\mathrm{FRM}} = -\bar{\rho}C_L u_\Delta'\Delta\frac{\partial \tilde{c}}{\partial x_i} - \rho_0 S_L M_i(\bar{c} - \tilde{c}), \qquad (7)$$

$$C_L = 0.12, \quad M_i = -\frac{\nabla\tilde{c}}{|\nabla\tilde{c}|}, \; u_\Delta' = \sqrt{(\widetilde{u_i u_j} - \widetilde{u_i}\widetilde{u_j})/3}$$

Further variants of this model have been investigated in Gao et al. (2015 a,b) and are not repeated here.

ANALYSIS AND RESULTS

The DNS data has been filtered with a Gaussian filter kernel $G(r) = (6/\pi\Delta^2)^{3/2}\exp(-r^2/\Delta^2)$. Results will be presented from $\Delta \approx 0.4\,\delta_{th}$ where the flame is almost resolved, up to $\Delta \approx 2.8\,\delta_{th}$ where the flame becomes fully unresolved and Δ is comparable to the integral length scale. The test filter takes the following simple form with $(a_{d-1}, a_{d0}, a_{d1}) = (C, 1-2C, C)$ where C is a free parameter with $C \le 1/3$:

$$\hat{f}_{i,j,k} = \sum_{di,dj,dk=-1,1} a_{di}\cdot a_{dj}\cdot a_{dk}\cdot f_{i+di,j+dj,k+dk} \qquad (8)$$

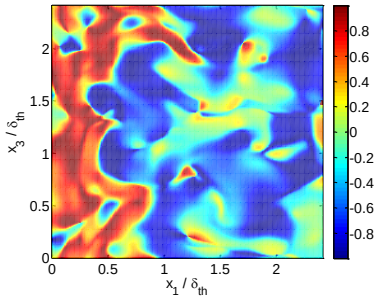

Figure 2: Instantaneous view of cosine of the angle Θ between scalar flux $\overline{\rho \boldsymbol{u} c} - \bar{\rho}\widetilde{\boldsymbol{u}}\tilde{c}$ from DNS and $-\nabla\tilde{c}$ for case A1 and $\Delta \approx 1.6\delta_{th}$.

Figure 2 shows the local distribution of the cosine of the angle Θ between sgs scalar flux $\overline{\rho \boldsymbol{u} c} - \bar{\rho}\widetilde{\boldsymbol{u}}\tilde{c}$ evaluated from DNS and $-\nabla\tilde{c}$ for one filter width ($\Delta \approx 1.6\delta_{th}$) for case A1 and the same quantity conditioned on the Favre averaged progress variable $\tilde{c}$ for cases A1, D1, A2, D2 and four filter widths is shown in Fig. 3. For gradient transport (CGT) this angle would be zero (-180°) and the cosine of the angle would assume the value 1.0 (-1.0). The competing effects of heat release and turbulent velocity fluctuations can clearly be seen from Fig. 3. If the effects of heat release dominate over the effects of turbulence CGT is promoted. This can be best seen for *Le*=0.34 (i.e. case A1). This is due to the fact that flames with $Le \ll 1$ exhibit high rate of burning as a result of thermo-diffusive instabilities. Similarly, the probability for negative cosine values is considerably higher for the cases with low turbulence intensity, e.g. case A2. Conversely, if turbulence effects are strong relative to heat release gradient type transport becomes stronger and the amount

of CGT is reduced in cases D1,D2 (as well as E1 and E2 not shown). Negative cosine values are in all cases found in particular in the region corresponding roughly $0.2 \leq \tilde{c} \leq 0.8$ where the effects of heat release are most pronounced. Finally, it can be observed that the amount of CGT increases with increasing filter width.

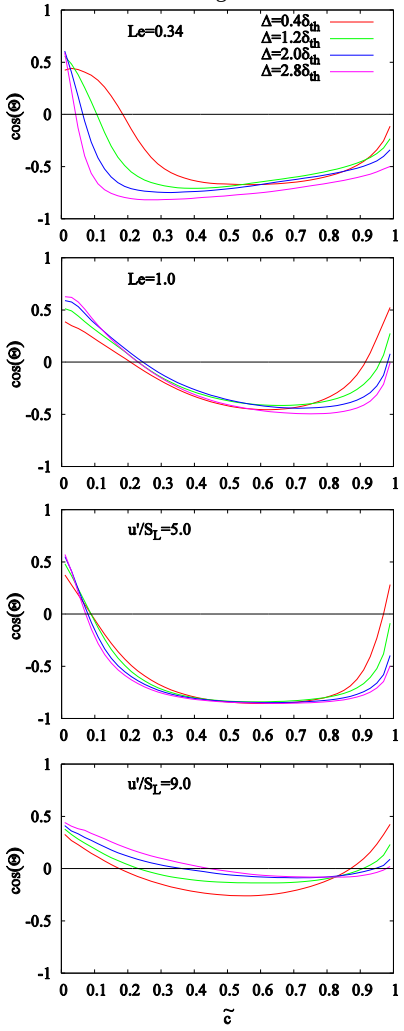

Figure 3. Cosine of angle Θ between $\overline{\rho \boldsymbol{u} c} - \bar{\rho}\tilde{\boldsymbol{u}}\tilde{c}$ calculated from DNS and $-\nabla\tilde{c}$ conditional on $\tilde{c}$ for cases A1, D1, A2, D2 for four different filter width.

Before the model performance will be analyzed in detail a preliminary test regarding the sensitivity of the results in response to details of the secondary filtering, i.e. the parameter C in eq. (8) will be discussed. The sensitivity on details of the filtering is not very pronounced for the VSS model and the DSS model. The VSS model shows the best performance in an intermediate range of the filter parameter C whereas the density based scale similarity model DSS shows slightly better results for larger C values corresponding to larger test filter width. In contrast the ASS model has a more pronounced sensitivity on details of test filtering and shows the best performance for smaller values of C for the current database. This can be understood from the fact that the second term in eq. (5) contains the expression $\overline{u_j'} = \overline{u_j} - \widehat{\overline{u_j}}$ which quickly approaches zero if the region of the intermediate scales becomes more and more narrow. As a result of this, the model is dominated by the first term on the r.h.s. of eq. (5) which looks similar to a scale similarity model. Based on the findings in Table 2 the filter parameter is set to $C = 1/6$ for the density based scale similarity model, whereas $C = 1/32$ is used in the ASS model. The VSS model is run with an intermediate model parameter of $C = 1/16$.

Table 2. Correlation strength between modelled flux and DNS flux for cases A1-E1 in dependence of the secondary filter parameter C. Correlation coefficients in direction of mean flame propagation (Corr1) and normal to it (Corr23) are averaged over all cases and all filter width.

	VSS		***DSS***		***ASS***	
	$corr_1$	$corr_{23}$	$corr_1$	$corr_{23}$	$corr_1$	$corr_{23}$
$\frac{1}{6}$	0.56	0.70	0.79	0.70	0.41	0.54
$\frac{1}{12}$	0.60	0.71	0.78	0.68	0.54	0.66
$\frac{1}{16}$	0.60	0.71	0.78	0.67	0.57	0.69
$\frac{1}{24}$	0.61	0.70	0.76	0.66	0.60	0.71
$\frac{1}{32}$	0.61	0.70	0.76	0.65	0.60	0.71

Figure 4 shows the correlation coefficients between scalar flux from DNS and different model expressions plotted against Δ/δ_{th} for cases A1,D1,A2,D2. It can be observed that the correlation strength decreases in all cases with increasing filter width. For the scale similarity type models (i.e. VSS, DSS, ASS, CGM, EGM) the correlation coefficient approaches unity in the limit of zero filter size. The results named CVSS and CASS correspond to the VSS and ASS model, but a conventional convolution filter is used for the second filter level rather than a Favre filter. The correlation coefficient of the gradient hypothesis model is small in magnitude for all cases and all filter width and has opposite sign in comparison to the DNS data. The FRM model shows a weaker dependency on the filter width but has a more pronounced dependency on Le as well as u'/S_L. The FRM correlation coefficients tend to be better when the heat release is strong relative to effects of turbulence (cases A1,B1,A2,B2) and in the direction of mean flame propagation x_1 (first column). Looking at the correlation coefficients $Corr_1$ shows also that taking care of density effects either by using Favre filtering or by including additional terms involving density in the CGM model improves considerably the magnitude of $Corr_1$ in particular for large filter width. Therefore the EGM is always superior to the CGM model and the Favre filtered scale similarity model versions perform better compared to their convolution filter counterparts. Conversely, turbulence effects have a stronger influence in direction normal to mean flame propagation (second column) and as a result the correlation coefficients $Corr_{23}$ of the VSS, DSS, ASS, CGM and EGM models lie within a much narrower band. Cases B2,B3,B5,A2,A3,A5 are not shown

for the sake of brevity, but the results follow the same trends, indicated by the discussion above.

The scale similarity models suffer from an insufficient amount of dissipation. In addition to the unsteady and advection terms, the transport equation for the progress variable variance in premixed flames contains the molecular diffusion, turbulent transport, reaction rate contribution, molecular dissipation terms and finally a term responsible for production or destruction of variance by mean gradients which is given by

$$Term_{PD} = \rho(\widetilde{u_i c} - \tilde{u}_i \tilde{c})\partial\tilde{c}/\partial x_i \qquad (9)$$

Hence it is interesting to study the correlation between the modelled expression for $Term_{PD}$ and the corresponding exact value. It can be observed in the third column of Fig.4 that some of the directional advantages and disadvantages of the models observed at the vector level are directly transferred to the scalar level when looking at $\bar{\rho}(\widetilde{u_i c} - \tilde{u}_i \tilde{c})\partial\tilde{c}/\partial x_i$. This is due to the fact that the mean value of $\nabla\tilde{c}$ is aligned with the direction of mean flame propagation and hence taking the scalar product of the sgs scalar flux with the gradient of $\tilde{c}$, does nothing else other than selecting predominantly the x_1 component of the scalar flux.

The correlation coefficient considered so far provides local information about the fluctuation and alignment of scalar flux and the corresponding model expression. However, it is only a measure of linear dependence between two quantities and hence invariant under multiplication of the model with a constant. The second step in the analysis is therefore to compare the magnitude of modelled scalar flux with the magnitude of its corresponding DNS value. In the context of scalar flux modelling for turbulent premixed flames the scalar flux model has to work well on the product side as well as on the reactant side and of course within the flame front. In each of these regions the model has to represent the scalar flux for different conditions and for different physical mechanisms. Therefore the approach adopted in this work is to present the scalar flux as a mean value conditional on the Favre averaged progress variable $\tilde{c}$.

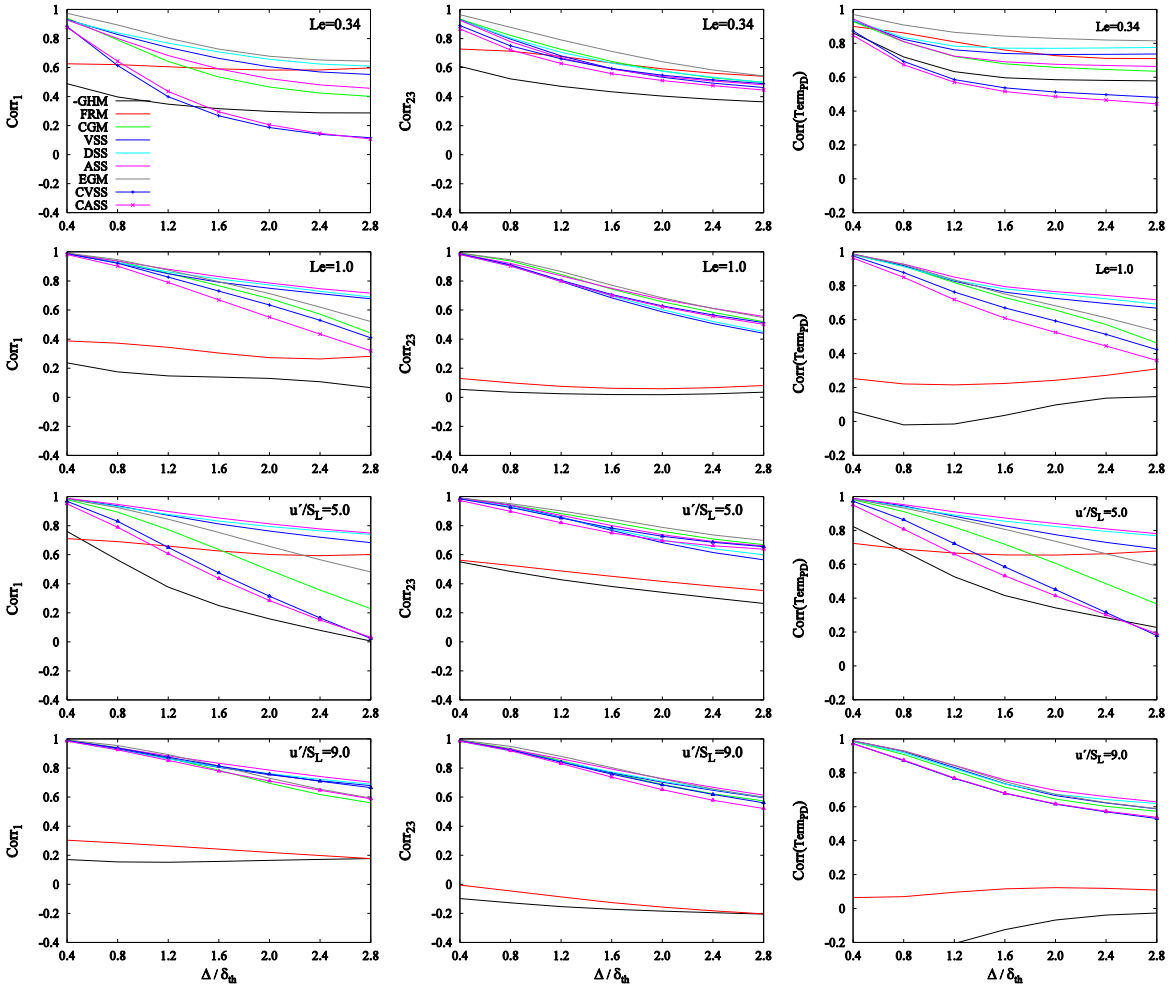

Figure 4. Correlation coefficients between scalar flux $\overline{\rho \boldsymbol{u} c} - \bar{\rho}\tilde{\boldsymbol{u}}\tilde{c}$ calculated from DNS and different model expressions in direction of mean flame propagation ($Corr_1$, first column) and normal to it ($Corr_{23}$, second column) plotted against Δ/δ_{th} for cases A1,D1,A2,D2. The correlation coefficients of the GHM model are multiplied with -1. The corresponding correlations for $Term_{PD}$ are shown in the last column.

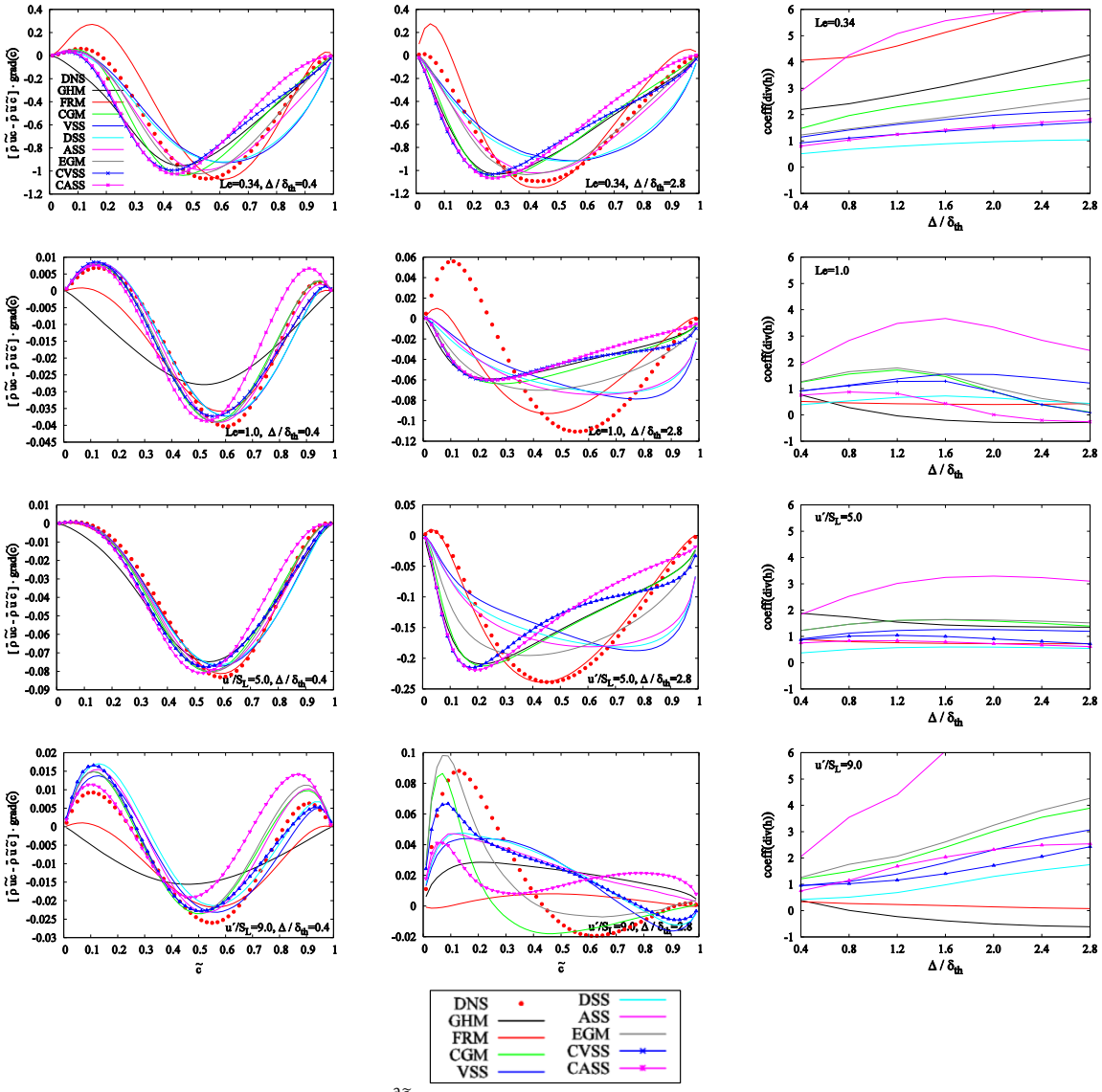

Figure 5. Conditional plot of $(\overline{\rho u_i c} - \bar{\rho}\widetilde{u_i}\tilde{c})\frac{\partial \tilde{c}}{\partial x_i}$ calculated from DNS as well as different model expressions against $\tilde{c}$ for $\Delta \approx 0.4\delta_{th}$ (first column) and $\Delta \approx 2.8\delta_{th}$ (second column) for cases A1,D1,A2,D2. Leading model coefficients are optimized using a least square approach and are shown in the third column.

In contrast to the correlation analysis this comparison depends on model coefficients which have the form of a leading multiplier. The goal of a-priori analysis is to identify potentials of a model but the final assessment has to be done in a-posteriori analysis. Instead of a dynamic evaluation, which typically comes along with a rather complex regularization procedure, a simpler approach is therefore adopted in this work and an optimal model multiplier is determined by a least squares fit of the two curves representing $Term_{PD}$ evaluated from DNS respectively its model representation conditional on $\tilde{c}$. The resulting conditional plots can be seen in the first two columns of Fig. 5. The third column in Fig. 5 shows the optimal multipliers used for these plots. The GHM model is multiplied with a negative model constant and needs no further discussion. The FRM model performs remarkably well for cases with

Lewis numbers up to $Le = 0.8$ and for initial turbulence intensities up to $u'/S_L = 6.25$ (see e.g cases A1,A2). The other models show a satisfactory behavior for small filter width. However, no model gives reliable predictions throughout the whole parameter range. Ideally, the model multiplier shown in the third column of Fig, 5 would be unity, but at least constant for all filter width and all cases considered. If these criteria are not met it seems to be desirable if the model multiplier approaches an asymptotic value for large filter width. Among the models considered here these requirements seem to be best met by the DSS model. The model multipliers with a significant change in magnitude indicate the need for either a case to case adaption of the model parameter or even a local evaluation of model parameters.

CONCLUSIONS AND FUTURE OUTLOOK

The main findings can be summarized as follows: 1.The gradient hypothesis model is for all cases and filter width poorly, and mostly negatively, correlated with the scalar flux. 2. The FRM shows small values of correlation coefficients except for situations where heat release dominates over the effects of turbulence. 3. Despite the fact that all scale similarity type models used in this work have been developed in the context of non-reactive flow, they are rather successful in representing the SGS scalar flux for turbulent premixed flames. The same holds true for the CGM model. 4. All SS type models are sensitive to details of test-filtering. The strongest sensitivity was found for the ASS model which required rather narrow test filter width. Test filtering with a Favre filter resulted in considerable improvements of the correlation strength in direction of mean flame propagation for the VSS and ASS models. 5. The CGM model can be improved by including additional higher order terms which involve gradients of density. A new EGM model was suggested on an empirical basis that performs in all cases better than the CGM model. 6. All models, except GHM and FRM, perform similar in direction normal to mean flame propagation but there are more pronounced differences in direction of mean flame propagation.

It is common understanding that a-priori analysis can help to show potentials of LES models, but that the models need to be implemented in an LES code, ideally using complex chemistry, for final assessment. Overall the SS type models show very good performance and seem to be promising candidates for such a-posteriori analysis.

ACKNOWLEDGEMENTS

YG and NC are grateful to EPSRC, UK. MK is thankful to J.A. Domardzki for several fruitful discussions.

REFERENCES

B.W. Anderson and J.A. Domaradzki (2012), A sub-grid model for large eddy simulation based on the physics of interscale energy transfer in turbulence, Physics of Fluids, Vol. 24, 065104.

Chakraborty, N., Katragadda, M., Cant, R.S. (2011a) Effects of Lewis number on turbulent kinetic energy transport in turbulent premixed combustion, Phys. Fluids, 23, 075109.

Chakraborty, N., Hartung, G., Katragadda, M., Kaminski, C. F. (2011b). A numerical comparison of 2D and 3D density-weighted displacement speed statistics and implications for laser based measurements of flame displacement speed, Combust. Flame, Vol. 158, pp. 1372-1390.

Gao, Y., Chakraborty N. and Klein, M. (2015a), Assessment of the performances of sub-grid scalar flux models for premixed flames with different global Lewis numbers: A Direct Numerical Simulation analysis, International Journal of Heat and Fluid Flow, Vol. 52, pp.28-39.

Gao, Y., Chakraborty N. and Klein M. (2015b), Assessment of sub-grid scalar flux modelling in premixed flames for Large Eddy Simulations: A-priori Direct Numerical Simulation analysis, European Journal of Mechanics - B/Fluids, in press.

Richard, S., Colin, O., Vermorel, O., Angelberger, C., Benkenida, A., Veynante, D. (2007), Large eddy simulation of combustion in spark ignition engine, Proc. Combust. Inst., Vol. 31, pp. 3059–3066.

Sagaut, P. (1998), Large Eddy Simulation for incompressible Flow, Springer Berlin Heidelberg.

Veynante D., Trouvé A., Bray K.N.C., Mantel T. (1997) Gradient and counter-gradient turbulent scalar transport in turbulent premixed flames, J. Fluid Mech., 332, 263-293.

Vreman B. (1995) Direct and Large Eddy Simulation of the Compressible Mixing Layer, PhD Thesis, University of Twente.